

# Design Parameter for Assessing Wicking Capabilities of Heat Pipes

F.C. Yip\*

*Communications Research Centre, Ottawa, Canada*

The increasing use of heat pipes as efficient thermal power-transfer devices for the thermal control of high-power communication satellites suggests that there is a need for some parametric index to compare the thermal characteristics of different heat pipe structures. It is shown that the maximum heat-transfer rate sustainable by a heat pipe with a given working fluid is proportional to a wick parameter  $N_w$ , which is a function of the wick geometry and structural design alone. Expressions for  $N_w$  are derived and numerical values are tabulated for various wick structures used in heat pipe applications. Validity of this parameter is confirmed by comparison with over 70 measurements gathered from various sources. It is also shown that  $N_w$  may be evaluated for heat pipes with composite wick structures, and an example is given.

## Nomenclature

$A_t$	= cross-sectional area of liquid-flow channel
$b$	= width of grooves
$D_t$	= equivalent hydraulic diameter
$D_p$	= particle diameter
$g$	= gravitational constant
$h_{lv}$	= latent heat of evaporation
$i, j$	= summation indices
$K_p$	= wick permeability
$\ell$	= length
$\ell_m$	= effective transport length
$\ell_t$	= total heat pipe length
$\ell_w$	= width of wick, or nominal inside circumference of heat pipe
$M$	= number of wick sections
$N$	= number of wick layers
$N_\ell$	= liquid parameter [Eq. (11)]
$N_w$	= wick parameter (Fig. 3)
$\Delta P_G$	= gravitational pressure force
$\Delta P_\ell$	= pressure drop in liquid phase
$\Delta P_s$	= capillary pumping pressure
$Q$	= heat-transfer rate
$r_c$	= equivalent minimum meniscus radius
$t_w$	= wick thickness
$\alpha_p$	= groove pitch ratio, $\text{pitch}/b$
$\alpha_w$	= groove depth ratio, $t_w/b$
$\epsilon$	= porosity
$\mu_\ell$	= liquid viscosity
$\rho_\ell$	= liquid density
$\sigma$	= surface tension
$\phi$	= angle of inclination
$\theta$	= contact angle
$\psi$	= gravity factor [Eq. (9)]

## Subscripts

$a$	= adiabatic section
$c$	= condenser end
$e$	= evaporator end
$i, j$	= indices
max	= maximum value

Presented as Paper 74-1266 at the CASI/AIAA Joint Meeting, Toronto, Canada, October 30-31, 1974; submitted November 18, 1974; revision received July 29, 1975. The support of the spacecraft mechanics staff at CRC is appreciated.

Index category: Spacecraft Temperature Control Systems.

\*Research Scientist, Department of Communications. Member AIAA.

## I. Introduction

THE heat pipe has recently become one of the most versatile devices in the field of thermal control.<sup>1</sup> In a heat pipe, the thermal energy is absorbed at one end by a vaporization process and is rejected at the other end by a condensation process. The condensate is returned to the evaporator end by means of capillary forces provided by some form of wick inside the heat pipe. Large thermal loads can be transported over long distances with only a small temperature drop. The heat pipe, therefore, provides a very low thermal impedance between the heat source and the heat sink. Since the return of the condensate requires no mechanical pump or other means that may consume energy, a heat pipe may be operated for long lifetimes with little mechanical wear and maintenance if compatible materials and fluids are employed and a proper wick is provided. In view of its low thermal impedance, ability to transfer a high heat flux, low maintenance requirements, high reliability,<sup>2</sup> and light weight, the heat pipe is particularly suitable for space applications.<sup>3-6,27,30</sup>

At present there exists neither an easy method for assessing the merit of the wicking materials or structures nor a general guideline for the design of the wick structure. This makes it difficult to select the proper wick structure of a heat pipe to meet the design requirements. It is, therefore, the intent of the present work to propose a simpler parameter by which the merits of wicks can be characterized. Various wicking materials and structures are considered here, namely: wire cloths, metallic fibers, reffrasil cloths, packed particles, and covered and uncovered grooves of three different shapes. It will be demonstrated that this new parameter can easily be applied to predict the heat-transfer capacity of a specific type of composite wick heat pipe.

## II. Heat-Transfer Limit

The general criterion for determining the heat-transfer limit of a heat pipe is to equate the sum of pressure drops in the liquid phase and vapor phase to the maximum capillary pumping pressure and the pressure due to gravity, which may aid or act against the flow of the liquid.

Fig. 1 presents the model for the present analysis. It shows a single wick, which is saturated with liquid. Heat  $Q$  is being added at one end and removed at the other. It is assumed that there is a closed and continuous circulation of vapor between the two ends and that the vapor passage is unrestricted. This assumption makes it possible to neglect the pressure loss in the vapor phase.

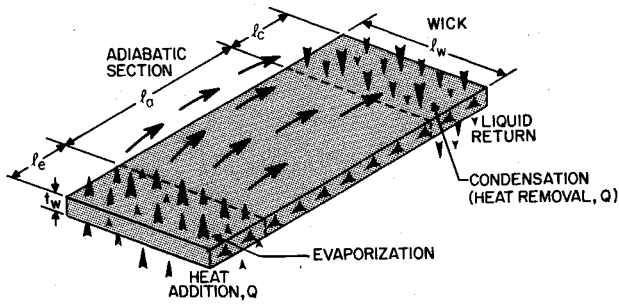


Fig. 1 Simple model for analyzing heat pipe wick.

### Liquid Pressure Drop

a) Porous materials: The steady-state pressure drop in the liquid phase may be approximated by

$$\Delta P_t = -\mu_t Q \ell_m / K_p \rho_t \epsilon \ell_w t_w h_{tw} \quad (1)$$

with uniform heating and cooling,<sup>7</sup> where  $\ell_m$  is the effective transport length, which is equivalent to  $(\ell_e + \ell_c)/2$  for the evaporator and condenser sections. For the adiabatic section, i.e., the thermally insulated portion of the heat pipe, the effective length will be taken to be the total length of the section. Equation (1) also assumes that Darcy's law applies, which may be justified if the flow considered is laminar.<sup>22</sup> This is the case for most heat pipe applications. Note that the effective permeability was used in Ref. 22, which is simply a product of  $\epsilon$  and  $K_p$ .

b) Grooves or channels: Under the same flow condition as stated earlier, the expression for the pressure drop in the liquid phase may be derived, based on the simple hydraulic consideration,<sup>13</sup> and is given by

$$\Delta P_t = -32\mu_t Q \ell_m / \rho_t h_{tw} A_t D_t^2 \quad (2a)$$

with

$$D_t = 4A_t / \text{wetted perimeter} \quad (2b)$$

where  $D_t$  is the equivalent hydraulic diameter and  $A_t$  is the cross-sectional area of the flow passage.

### Maximum Capillary Pumping Pressure

The capillary pressure force is generally described by means of Young's equation in the following form

$$\Delta P_s = 2\sigma [(\cos \theta_1 / r_{c1}) - (\cos \theta_2 / r_{c2})] \quad (3)$$

where  $\theta_1$  and  $\theta_2$  are the contact angles, and  $r_{c1}$  and  $r_{c2}$  are the meniscus radii of the vapor-liquid interfact at the extreme ends of the evaporator and condenser respectively. The meniscus radius is largest at the condenser end and smallest at the evaporator end. The contact angle  $\theta$  approaches zero if excellent wetting of the wick by the liquid is obtained.

The capillary pressure force given by Eq. (3) is the primary driving force available for returning the condensed working fluid to the evaporator end. It approaches a maximum value when  $\theta_1 = 0$  deg and  $\theta_2 = 90$  deg,  $r_{c1}$  becomes minimum and  $r_{c2}$  becomes infinitely large. Hence, from Eq. (3) the maximum capillary pressure force becomes

$$(\Delta P_s)_{\max} = 2\sigma / r_c \quad (4)$$

where  $r_c$  is the effective minimum meniscus radius, which has been found to depend primarily on the mesh size and pore radius of the wicking material,<sup>18</sup> or on the dimension of the flow channel for the case of grooved heat pipes.<sup>19</sup> For porous wick,  $r_c$  can be approximated by the effective pore radius of

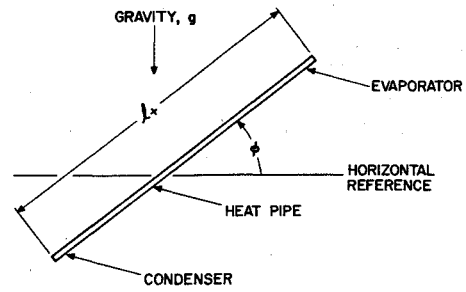


Fig. 2 Heat pipe at inclined position.

the wick.<sup>18</sup> For the case of grooves heat pipes,  $r_c$  is given by the following equation<sup>19</sup>

$$r_c = 2A_t / (\text{wetted perimeter} - b) \quad (5)$$

where  $b$  is the width of the grooves.

### Gravitational Pressure Force

However, if the heat pipe is inclined at an angle  $\phi$ , as shown in Fig. 2 and is subject to the influence of gravity, it is necessary to account for the effect of gravity. The gravitational pressure force exerted on the working fluid is given by

$$\Delta P_G = \ell_t \rho_t g \sin \phi \quad (6)$$

This equation does not account for the component of the gravitational force acting around the circumference of a wrapped structure.

### Heat-Transfer Capacity

By balancing the available pumping pressure, the gravitational pressure force as given by Eq. (4) and (6), respectively and the pressure loss in the liquid phase, as described by Eq. (1) or (2a), one obtains the following result:

$$Q_{\max} = \psi (h_{tw} \sigma \rho_t / \mu_t) (2K_p \epsilon \ell_w / r_c) (\ell_w / \ell_m) \quad (7)$$

for porous wick and

$$Q_{\max} = \psi (h_{tw} \sigma \rho_t / \eta_t) (A_t D_t^2 / 16 \ell_w r_c) (\ell_w / \ell_m) \quad (8)$$

for grooves or channel wick

where

$$\psi = 1 - (r_c \ell_t \rho_t g \sin \phi / 2\sigma) \quad (9)$$

is a correction factor for the gravity effect. It becomes unity when the heat pipe is operated in zero gravity or at zero tilt in a terrestrial environment.

Equations (7) and (8) represent the heat-transfer capacity of the heat pipe wick which must not be exceeded in the operation of a heat pipe; otherwise, burnout of the evaporator could occur.

Equations (7) and (8) can be further simplified to the following form:

$$Q_{\max} = \psi N_t N_w (\ell_w / \ell_m) \quad (10)$$

where  $N_t$  is the liquid parameter given by

$$N_t = h_{tw} \sigma \rho_t / \mu_t \quad (11)$$

and is a measure of the merit of the working fluid.<sup>7,13,16,17</sup> The liquid parameter as defined by Eq. (11) depends on the thermophysical properties of the working fluid and is, therefore,

Table 1 Values of  $N_w$  for various wick structures

Type		$K_p$ ( $10^{-8}\text{ft}^2$ )	$\epsilon$	$t_w$ (in.)	$r_c$ (in.)	$N_w$ ( $10^{-8}\text{ft}^2$ )	Refer- ence	Supplier
Copper	210-5	2.80	0.945	0.018	0.018	5.28	8	Astro Met Associates Inc.
Foam	220-5	3.00	0.912	0.102	0.019	29.4	8	Astro Met Associates Inc.
Nickel	210.5	3.95	0.944	0.102	0.018	42.3	8	Astro Met Associates Inc.
Foam	220-5	5.00	0.960	0.100	0.019	50.5	8	Astro Met Associates Inc.
Copper	1005	1.25	0.895	0.100	0.019	11.8	8	Astro Met Associates Inc.
Felt		0.0464	0.59	0.065	0.0016	2.24	24	Huyck Metals Co.
		0.196	0.80 (0.20) <sup>a</sup>	0.125	0.0036	10.9 (11.1)	25	Huyck Metals Co.
Nickel	Felt 1210 1212	0.60	0.891	0.101	0.013	8.31	8	Astro Met Associates Inc.
		0.0650	0.82	0.076	0.0017	7.43	24	Huyck Metals Co.
		0.0089	0.61	0.083	0.00085	1.05	24	Huyck Metals Co.
		0.122	0.85	0.125	0.0026	9.97 (9.81)	25	Huyck Metals Co.
		(0.120) <sup>a</sup>	0.067	0.80	0.125	6.38 (6.57)	25	Huyck Metals Co.
		(0.069)	0.017 (0.023)	0.70	0.125	1.98 (2.68)	25	Huyck Metals Co.
Stain- less steel	1306	0.642	0.89	0.120	0.0073	18.79	24	Huyck Metals Co.
	1307	0.290	0.80	0.128	0.0041	14.42	24	Huyck Metals Co.
Felt	1308	0.0592	0.58	0.128	0.0019	4.58	24	Huyck Metals Co.
Sintered	H1	0.0472	0.868	0.0825	0.0014	4.83	7	
Nickel	H2	0.0362	0.825	0.0825	0.0014	3.52	7	
Fiber	H3	0.0163	0.689	0.0825	0.0014	1.32	7	
	H6	0.0332	0.880	0.0825	0.0014	3.44	7	
Sintered	H11	0.59	0.916	0.0991	0.0037	29.0	7	
Steel	H12	0.21	0.808	0.0991	0.0025	13.5	7	
Fiber	H13	1.25	0.822	0.0991	0.0043	47.4	7	
Sintered	M2	0.294	0.658	0.0873	0.0023	14.7	7	
Nickel	M4	0.087	0.540	0.540	0.0014	5.86	7	
Powder	M6	0.323	0.696	0.0873	0.0033	11.9	7	
Sintered	1845-137	0.00515	0.62	0.031	0.00057	0.347	24	Huyck Metals Co.
Copper	1845-138	0.00643	0.70	0.030	0.00060	0.450	24	Huyck Metals Co.
Powder	1845-139	0.00608	0.57	0.051	0.00058	0.609	24	Huyck Metals Co.
Sintered	3M-2M	0.00534	0.32	0.112	0.00048	0.797	24	Huyck Metals Co.
Steel	3M-3M	0.0177	0.47	0.111	0.00092	2.01	24	Huyck Metals Co.
Powder	3M-4MX	0.0460	0.57	0.118	0.0016	3.87	24	Huyck Metals Co.
Packed particles								
Type		$K_p$ ( $10^{-8}\text{ft}^2$ )	$\epsilon$	$t_w$ (in.)	$r_c$ (in.)	$N_w$ ( $10^{-8}\text{ft}^2$ )	Reference	Supplier
Glass beads	20-30 mesh	1.04	0.43	0.467 <sup>c</sup>	0.0051	82.1	24	
	30-40 mesh	0.758	0.40	0.467	0.0037	76.3	24	
	40-50 mesh	0.321	0.41	0.467	0.0026	47.6	24	
	60-70 mesh	0.119	0.39	0.467	0.0015	28.3	24	
	70-80 mesh	0.108	0.38	0.467	0.0014	27.0	24	
	80-100 mesh	0.0754	0.40	0.467	0.0011	26.8	24	
Covered grooves								
Type		$\alpha_w$	$\alpha_p$	$b$ (in.)	$r_c$ (in.)	$N_w$ ( $10^{-8}\text{ft}^2$ )	Refer- ence	
Rectangular		2.50	3.52	0.0063	0.0032	4.92	11	
		2.50	2.81	0.0079	0.0032	12.1	11	
		1.25	3.17	0.0158	0.0032	26.0	11	
		2.50	4.73	0.0047	0.0032	1.52	11	

Table 1 continued

Table 1 Continued								
Shallow channel								
	Type	$K_p$ ( $10^{-8} \text{ ft}^2$ )		$t_w$ (in.)	$r_c$ (in.)	$N_w$ ( $10^{-8} \text{ ft}^2$ )	Refer- ence	Supplier
Wire Cloths	200 mesh	0.0800	0.733	0.0035	0.0022	0.187	8	Michigan Wire Cloth Co.
	200 mesh	0.0834	0.676	0.0044	0.0025	0.198	7	
	150 mesh	0.110 <sup>e</sup>	0.678	0.0060	0.0033	0.271	7	
	100 mesh	0.164	0.679	0.0090	0.393	7		
	50 mesh	0.715	0.625	0.0180	0.0119	1.35	7	Gerard Daniel and Co.
	200 mesh	0.0587	0.69	0.0035 <sup>e</sup>	0.0025	0.113	24	
	150 mesh	0.0865	0.68	0.0060 <sup>e</sup>	0.0035	0.202	24	
	100 mesh	0.222	0.63	0.0090 <sup>e</sup>	0.0045	0.559	24	
	40 mesh	0.397	0.69	0.0180 <sup>e</sup>	0.0091	1.08	24	
	125 mesh	0.154	0.60	0.125 <sup>a</sup>	0.0046	5.02	25	
		(0.105 <sup>a</sup> )				(3.42)		
	200 mesh	0.0493	0.67	0.0033	0.00125	0.174	29	
325 mesh	0.0316	0.67	0.0028	0.00084	0.141	29		
Porous materials								
	Type	$K_p$ ( $10^{-8} \text{ ft}^2$ )	$\epsilon$	$t_w$ (in.)	$r_c$ (in.)	$N_w$ ( $10^{-8} \text{ ft}^2$ )	Refer- ence	Supplier
Refrasil sleeving	b1/2	0.255	0.40	0.032	0.0064	1.02	9	Hitco
Refrasil cloth	C100-28			0.014		0.238 <sup>b</sup>	21	Hitco
Grooves								
	Type	$\alpha_w$	$\alpha_p$	$b$ (in.)	$r_c$ (in.)	$N_w$ ( $10^{-8} \text{ ft}^2$ )	Refer- ence	Supplier
Rectangular		1.17	1.70	0.0300		52.8	12	French Tubing Co.
		2.50	3.52	0.0063		3.40	11	French Tubing Co.
		2.50	4.73	0.0047		1.41	11	
		2.50	2.81	0.0079		6.69	11	
		1.25	3.17	0.0158		8.72	11	
		1.60	1.60	0.0098		9.68	14	
		1.50	2.00	0.0158		18.3	14	
		1.16	1.44	0.0302		62.3	4	French Tubing Co.
		5.30	2.00	0.0129		63.9	13	
		3.84	2.00	0.0135		47.6	13	
		2.94	2.00	0.0160		47.7	13	
		2.38	2.00	0.0201		57.0	13	
		2.03	2.00	0.0260		76.7	13	
		1.54	1.84	0.0260		56.1	27	French Tubing Co.
Triangular		2.22	2.78	0.0045		0.534	30	Grumman Aerospace Corp.
Packed particles								
	Type	$K_p$ ( $10^{-8} \text{ ft}^2$ )	$\epsilon$	$t_w$ (in.)	$r_c$ (in.)	$N_w$ ( $10^{-8} \text{ ft}^2$ )	Refer- ence	Supplier
Monel beads		0.0297 <sup>c</sup>	0.40	0.467	14.3		10	
		0.0363 <sup>c</sup>	0.40	0.467	0.0084	15.8	10	
		0.128 <sup>c</sup>	0.40	0.467	0.0016	29.6	10	
		0.249 <sup>c</sup>	0.40	0.467	0.0022	41.3	10	
Monel beads	20-30 mesh	1.20	0.39	0.467 <sup>d</sup>	0.0054	80.4	24	
	30-40 mesh	0.792	0.42	0.467	0.0038	81.8	24	
	40-50 mesh	0.434	0.60	0.467	0.0031	79.0	24	
	50-60 mesh	0.182	0.50	0.467	0.0019	43.8	24	
		0.136	0.47	0.467	0.0016	40.1	24	
	70-80 mesh	0.0924	0.68	0.467	0.0015	39.4	24	
	80-100 mesh	0.0716	0.67	0.467	0.0012	36.4	24	
	100-140 mesh	0.0441	0.61	0.467	0.00091	27.6	24	
	140-200 mesh	0.0277	0.56	0.467	0.00074	19.6	24	

<sup>a</sup> Value in bracket was determined by means of the Siphon method. Number of layers of screen was not reported. <sup>b</sup> Measured value based on Eq. (10). <sup>c</sup> Calculated from Blake-Kozeny equation. <sup>d</sup> Estimated value based on Ref. (10). <sup>e</sup> Approximate value.

temperature dependent. In general, metals have the highest value of  $N_w$ , ranging from 400 to 2,000 Btu-lbf-hr/ft<sup>3</sup>-lbm. Among the nonmetallic fluids, which include organic and inorganic liquids, water has the largest value of  $N_w$ . Cryogenic fluids have the lowest values.

$N_w$  is defined here as the wick parameter given as follows

$$N_w = 2K_p \epsilon t_w / r_c \quad (12)$$

for porous wick, and

$$N_w = A_t D_t^2 / 16 \ell_w r_c \quad (13)$$

for groove or channel wick.

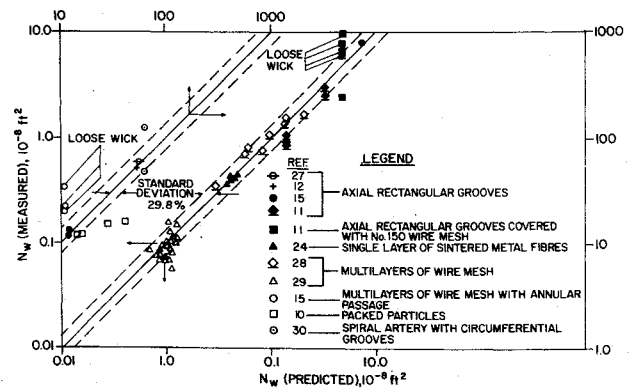
CLASS	DESCRIPTION	CONFIGURATION	$N_w$
1	POROUS MATERIALS		$N_w = \frac{2K_p \epsilon t_w}{r_c}$
			RECTANGULAR GROOVES $N_w = \frac{a_w^3 b^2}{a_p (1 + 2a_w)^2}$
			SEMICIRCULAR GROOVES $N_w = \frac{(\pi - 2)b^2}{64 a_p}$
			TRIANGULAR GROOVES $N_w = \frac{a_w^2 (\sqrt{1 + 4a_w^2} - 1)b^2}{8(1 + 4a_w^2)a_p}$
		where $a_w = t_w/b$ , $a_p = \text{Pitch}/b$ , see also Ref. (19)	
3	PACKED PARTICLES		$N_w = \frac{2K_p \epsilon t_w}{r_c}$ where $K_p = \frac{\epsilon^2 D_p^2}{150(1 - \epsilon)^2}$ Cubically Packed Particles: $r_c = 0.205 D_p$ (Ref. 18) Hexagonally Packed Particles: $r_c = 0.0775 D_p$ (Ref. 18)
			RECTANGULAR GROOVES $N_w = \frac{a_w^3 b^3}{4(1 + a_w)^2 a_p r_c}$ SEMICIRCULAR GROOVES $N_w = \frac{\pi^3 b^3}{128(2 + \pi)^2 a_p r_c}$ TRIANGULAR GROOVES $N_w = \frac{a_w^3 b^3}{8(1 + \sqrt{1 + 4a_w^2})^2 a_p r_c}$ where $a_w = t_w/b$ , $a_p = \text{Pitch}/b$ , $r_c = \text{Pore radius}$
5	SHALLOW CHANNEL		$N_w = \frac{t_w^3}{4 r_c}$ where $r_c = \text{Pore radius}$

Fig. 3 Expressions of  $N_w$  for various wick structures.

### III. Wick Parameter

The wick parameter  $N_w$  which was introduced in Eq. (10), is a measure of the heat-transfer capacity of the wick. Expressions of  $N_w$  are obtained, based on Eqs. (7) and (8), and are presented in Table 1 for other wick structures, which represent most of the basic types commonly used in the design of heat pipes. With the expressions of  $N_w$  presented herein, it is possible to estimate the capacity of each wick structure. For certain wick structures, however, the permeability and the porosity of the wick are required to determine  $N_w$ , and they must be determined experimentally.<sup>7,8,24</sup> Above all, one is required also to determine the effective meniscus radius by either experiments, or from Eq. (5), or the analytical model proposed by Tien and Sun.<sup>18</sup>

For comparison, Table 1 presents the analytical values of  $N_w$ , based on expressions given in Fig. 3, for a wide range of wick materials and structures which were used in the past investigations.<sup>4, 7-14, 21, 24, 25, 17, 29</sup> Note that most of the wick materials listed are commercially available. One may notice also that certain wick materials or structures are superior to others as regards their wicking capability. As an example, grooved wicks have large values of  $N_w$  compared to most simple porous wick structures. On the other hand, grooves which are covered with wire mesh are shown to have a significantly higher value of  $N_w$  than those which are uncovered.

Fig. 4 Comparison of measured and predicted  $N_w$ .

The validity of the proposed wick parameter can be established here by comparison with test data currently available. Based on the informations extracted from nine different sources,<sup>10-12,15,24,27-30</sup> the values of  $N_w$  are determined from Eq. (10). These are then compared with those calculated from the analytical expressions in Fig. 4 for a sample of more than 70 measurements taken on a variety of wick structures.

Good agreement is seen between the measurements and the predictions, as shown in Fig. 4. This is in spite of many uncertainties associated with the quality of the working fluids and the specimens, and the procedure in the measurement of the heat-transfer limit. The present theory is particularly good for the grooved heat pipes. Fig. 4 shows that only a small amount of test data deviates from the prediction by more than 30%. These large discrepancies are caused by problems associated with the manufacture of the wick, which could result in looseness in the wick or in a nonuniform size of the artery and flow channels. Improved quality control would attenuate this scatter.

### IV. Application

This section shows how the values of  $N_w$  can be extended to arrive at an overall wicking capability of a composite wick heat pipe.

#### Single Wick

By inspection, Eq. (10) is analogous to Ohm's law, which governs the electrical current flow in a conductor. Here,  $Q_{\max}$  is analogous to the electric current, the product of  $\psi$  and  $N_w$  is analogous to the voltage difference, and the product of  $N_w$  and  $\ell_w/\ell_m$  is analogous to the conductance.

#### Composite Wick

It is possible to extend this analogy, established for a single wick, to the case of a composite wick structure adjacent to the wall. Figure 5 shows the physical model of an arbitrary composite wick structure, and its equivalent circuit is shown in Fig. 6. The model is divided lengthwise into  $M$  sections, which are physically connected but each of which may have a different material or structure. Within each section the wick is further subdivided into  $N_i$  wick components, where  $i = 1, 2, 3, \dots, M$ . Based on the equivalent circuit of Fig. 6, one can obtain the following result

$$Q_{\max} = \psi N_c / \left[ \sum_{i=1}^M 1 / \sum_{j=1}^{N_i} (N_{wij} \ell_{wij} / \ell_{mi}) \right] \quad (14)$$

This equation is quite general and applies to a composite wick structure. The values of  $N_{wij}$  may be obtained from Table 1 and Fig. 3.

#### Example

An example is given to illustrate how Eq. (14) can be applied to the design of a composite wick heat pipe. The heat

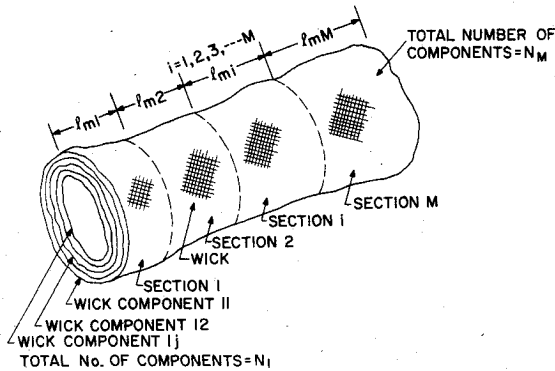


Fig. 5 Composite wick structure.

pipe is divided into three sections, i.e., evaporator, adiabatic, and condenser sections; thus  $M=3$ . Suppose the heat pipe wick is constructed using six layers of 200-mesh wire cloth. It is secured to the heat pipe wall at the evaporator and the condenser ends by means of retaining rings. Let us assume that there is a small amount of looseness<sup>†</sup> in the wick, say 0.0013 in. In the adiabatic section an annular passage with a clearance of 0.025 in. is provided between the wick and the heat pipe wall.

Let other details of the heat pipe construction be:  $\ell_e = 2$  in.,  $\ell_a = 16$  in.,  $\ell_c = 2$  in.,  $K_p = 8.0 \times 10^{-10}$  ft<sup>2</sup>,  $\epsilon = 0.733$ ,  $t_w = 0.0035$  in.,  $r_c = 0.0022$  in., radius of heat pipe wall = 0.438 in., total width of wire cloth = 16.5 in.

Now we can determine the overall wicking capability and the maximum heat-transfer limit of the heat pipe at no tilt condition, assuming, say, methanol as the working fluid at 100°C.

Based on the information just given, the value of  $N_w$  for each wick component is calculated from the corresponding expression of Fig. 3., as

for wire cloth

$$N_{w11} = N_{w21} = N_{w31} = 0.187 \times 10^{-8} \text{ ft}^2$$

for looseness

$$N_{w12} = N_{w22} = N_{w32} = 0.173 \times 10^{-8} \text{ ft}^2$$

for annular passage

$$N_{w23} = 0.123 \times 10^{-4} \text{ ft}^2$$

The effective lengths are given as follows:

$$\ell_{m1} = \ell_{m3} = \ell_e / 2 = 1.0 \text{ in.}$$

$$\ell_{m2} = 16.0 \text{ in.}$$

The widths of the wick components are  $\ell_{w11} = \ell_{w12} = \ell_{w21} = \ell_{w22} = \ell_{w31} = \ell_{w32} = 16.5$  in. and  $\ell_{w23} = 2.75$  in. Then, the overall wicking capability of this heat pipe can be determined Eq. (14), as follows

$$N_w \ell_w / \ell_m = 1 \left[ \sum_{i=1}^3 1 / \sum_{j=1}^{N_i} (N_{wij} \ell_{wij} / \ell_{mi}) \right]$$

where  $N_1 = 2$ ,  $N_2 = 3$ ,  $N_3 = 2$ . Hence,  $N_w \ell_w / \ell_m = 2.97 \times 10^{-8} \text{ ft}^2$ .

The liquid parameter  $N_\ell$  for the methanol at 100°C is approximately 32 Btu-lbf-hr/ft<sup>3</sup>-lbm.<sup>15</sup> Since there is no tilt,  $\psi$

<sup>†</sup>Looseness is defined here as the mean separation distance between the adjacent layers of material.

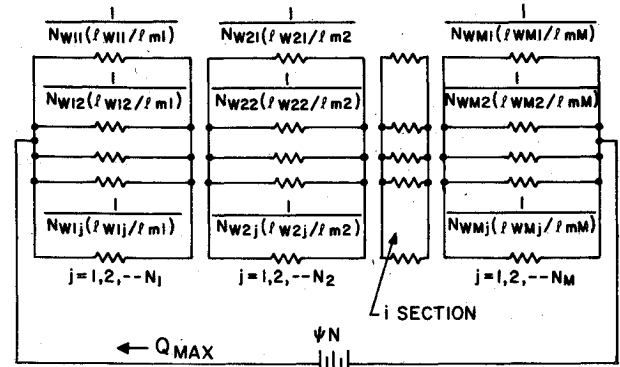


Fig. 6 Equivalent circuit of Fig. 5.

becomes 1.0. Thus, using Eq. (14), the limiting heat-transfer rate of this heat pipe is calculated to be 122 w.

This example demonstrates how the heat-transfer limit of the composite wick heat pipe can be determined when values of  $N_w$  for the individual wick structures are identified. This method is easily adaptable to the use of a digital computer, making it possible to calculate  $N_w$  readily for various wick structures, and to enable the selection of an optimal wick design for any particular heat pipe application.

## V. Conclusions

A wick parameter  $N_w$  has been derived which is useful for comparing the wicking capabilities of various heat pipe structures. The use of this parameter as a design tool is valid only if the vapor pressure drop is small and the liquid flow is laminar, which is usually the case.

Expressions and numerical values of  $N_w$  have been tabulated for various wick structures used in heat pipe applications. They show that wicks with rectangular grooves generally have large values of  $N_w$  compared to most simple wick structures, and that these values are even higher when the grooves are covered with wire cloths. The validity of  $N_w$  has also been confirmed for a number of wick structures by comparison with currently available measurements.

A formulation has been established to evaluate the overall wick capabilities of composite wick structures, and an example has been given to demonstrate the ease of its use.

## References

- Feldman, K.T. and Whiting, G.H., "Applications of the Heat Pipe," *Mechanical Engineering*, Vol. 11, Nov. 1968, p. 48.
- Basijulis, A. and Filler, M., "Operating Characteristics and Long-Life Capabilities of Organic Fluid Heat Pipes," *AIAA Progress in Astronautics and Aeronautics: Fundamentals of Spacecraft Thermal Design*, Vol. 29, edited by John W. Lucas, MIT Press, Cambridge, Mass., 1972, pp. 431-444.
- Hinderman, J.D., Madsen, J., and Waters, E.D., "An ATS-E Solar Cell Space Radiator Utilizing Heat Pipes," *AIAA Progress in Astronautics and Aeronautics: Thermophysics: Application of Thermal Design to Spacecraft*, Vol. 23, edited by Jerry T. Bevans, Academic Press, N.Y., 1970, pp. 405-422.
- Deverall, J.A. and Salami, E.W., "Heat Pipe Performance in a Zero Gravity Field," *Journal of Spacecraft*, Vol. 4, Nov. 1967, pp. 1556-1557.
- Harkness, R.E., "The Geos-II Heat Pipe System and Its Performance in Test and Orbit," Johns Hopkins University, Applied Physics Lab., Silver Spring, Md., Technical Memo, TG-1049, 1969.
- Franklin, C.A. and Davison, E.H., "A High-Power Communications Technology Satellite," *Progress in Astronautics and Aeronautics: Communications Satellite Systems*, Vol. 32, edited by P.L. Bargellini, MIT Press, Cambridge, Mass., 1974, pp. 87-121.
- Kunz, H.R., Langton, L.S., Hilton, B.H., Wyde, S.S., and Nashick, G.H., "Vapor Chamber Fin Studies-Transport Properties and Boiling Characteristics of Wicks," NASA CR-812, June 1967.
- Phillips, E.C. and Hinderman, J.D., "Determination of Properties of Capillary Media Useful in Heat Pipe Design," ASME Paper 69-Ht-18, 1969.

- <sup>9</sup>Farran, R.A. and Starner, K.E., "Determining Wicking Properties of Compressible Materials for Heat Pipe Applications," *Aviation and Space*, ASME Conference, June 16/19, 1968.
- <sup>10</sup>Cosgrove, J.H., Ferall, J.K., and Carnesalle, A., "Operating Characteristics of Capillarity-Limited Heat Pipes," *Journal of Nuclear Energy*, Vol. C21, 1967, pp. 547-558.
- <sup>11</sup>Kemme, J.E., "Heat Pipe Capability Experiment," Los Alamos Scientific Lab., N.M., 1966, Rept. LA-3585.
- <sup>12</sup>Kosowski, N. and Kosson, R., "Experimental Performance of Grooved Heat Pipes at Moderate Temperatures," AIAA Paper 71-409, Tullahoma, Tenn., 1971.
- <sup>13</sup>Frank, S., "Optimization of a Grooved Heat Pipe," *Advances in Energy Conversion Engineering*, ASME, New York, 1967, pp. 833-846.
- <sup>14</sup>Busse, C.A. et al., "Performance Studies on Heat Pipes," Thermionic Specialist Conference, 1967.
- <sup>15</sup>Yip, F.C., "An Experimental Study of Heat Pipes," Communications Research Centre, Ottawa, Canada, Tech. Rept., to be published.)
- <sup>16</sup>Handbook of Chemistry and Physics, Chemical Rubber Publishing Co., Cleveland, 1966-67 ed.
- <sup>17</sup>Glasstone, C., *Textbook of Physical Chemistry*, Van Nostrand, Princeton, N.J., 1946 (2nd ed.), p. 479.
- <sup>18</sup>Tien, C.L. and Sun, K.H., "Minimum Meniscus Radius of Heat Pipe Wicking Materials," *International Journal of Heat and Mass Transfer*, Vol. 14, Nov. 1971, pp. 1853-1855.
- <sup>19</sup>Bressler, R.G. and Wyatt, P.W., "Surface Wetting through Capillary Grooves," ASME Paper 68-Ht-19, 1969.
- <sup>20</sup>Soliman, M.M., Grauman, D.W., and Berenson, P.J., "Effective Thermal Conductivity of Dry and Water Saturated Sintered Fiber Metal Wicks," ASME Paper 70-HY/SPT-40, 1970.
- <sup>21</sup>Chato, J.C. and Streckert, J.H., "Performance of a Wick-Limited Heat Pipe," ASME Paper 69-HT-20, 1969.
- <sup>22</sup>Scheidegger, A.E., *The Physics of Flow through Porous Media*, MacMillan, New York, 1960.
- <sup>23</sup>Graumann, D.W., Richard, C.E., Duncan, J.D., Gibson, J.C., Coe, C.S., and Albright, C., "Research Study on Instrument Unit Thermal Conditioning Panel," NASA Rept. CR-103190, May 1971.
- <sup>24</sup>Ferrell, J.K. and Alexander, E.G., "Vaporization Heat Transfer in Heat Pipe Wick Materials, AIAA Paper 72-256, San Antonio, Texas, 1972.
- <sup>25</sup>Corman, J.C., Trefethen, L., and Walwet, G.E., "Characterization of Parameters for Liquid Flow in Rigid Porous Media," ASME Paper 73-WA/HT-3, 1973.
- <sup>26</sup>Seban, R.A. and Ahbat, A., "Steady and Maximum Evaporation from Screen Wicks," ASME Paper 71-WA/HT-12, 1971.
- <sup>27</sup>"ATS F&G Heat Pipe Critical Design Review," Dynatherm Corp., August 25-26, 1971.
- <sup>28</sup>Robert, C.C. and Feldman, K.T., "Predicting Performance of Heat Pipes with Partially Saturated Wicks," ASME Paper 72/WA/HT-39, 1972.
- <sup>29</sup>Chun, K.R., "Some Experiments on Screen Wick Dry-out Limits," *Journal of Heat Transfer*, Vol. 94, 1972, pp. 46-51.
- <sup>30</sup>Edelstein, F., Swerdling, B., and Kosson, R., "Development of a Self-Priming High-Capacity Heat Pipe for Flight on OAO-C," *AIAA Progress in Astronautics and Aeronautics: Thermal Control and Radiation*, Vol. 31, edited by Chang-Lin Tien, MIT Press, Cambridge, Mass., 1973, pp. 19-34.

## *From the AIAA Progress in Astronautics and Aeronautics Series . . .*

### **THERMAL CONTROL AND RADIATION—v. 31**

*Edited by C.-L. Tien, University of California, Berkeley*

Twenty-eight papers concern the most important advances in thermal control as related to spacecraft thermal design, and in radiation phenomena in the thermal environment of space, covering heat pipes, thermal control by other means, gaseous radiation, and surface radiation.

Heat pipe section examines characteristics of several wick materials, a self-priming pipe and development models, and the design and fabrication of a twelve-foot pipe for the Orbiting Astronomical Observatory C, and the 26-inch diode for the ATS-F Satellite.

Other thermal control methods examined include alloys, thermal control coatings, and plasma cleaning of such coatings. Papers examine the thermal contact resistance of bolted joints and electrical contacts, with role of surface roughness in thermal conductivity.

Gaseous radiation studies examine multidimensional heat transfer, thermal shielding by injection of absorbing gases into the boundary layer, and various gases as thermal absorbing media. Surface studies deal with real surface effects on roughened, real-time contaminated surfaces, and with new computational techniques to computer heat transfer for complex geometries, to enhance the capabilities and accuracy of radiation computing.

523 pp., 6 x 9, illus. \$12.95 Mem. \$18.50 List

TO ORDER WRITE: Publications Dept., AIAA, 1290 Avenue of the Americas, New York, N. Y. 10019